SINTEF
PROCEEDINGS
2

Proceedings of the 12th International Conference on Computational Fluid Dynamics in the Oil & Gas, Metallurgical and Process Industries

Progress in Applied CFD – CFD2017

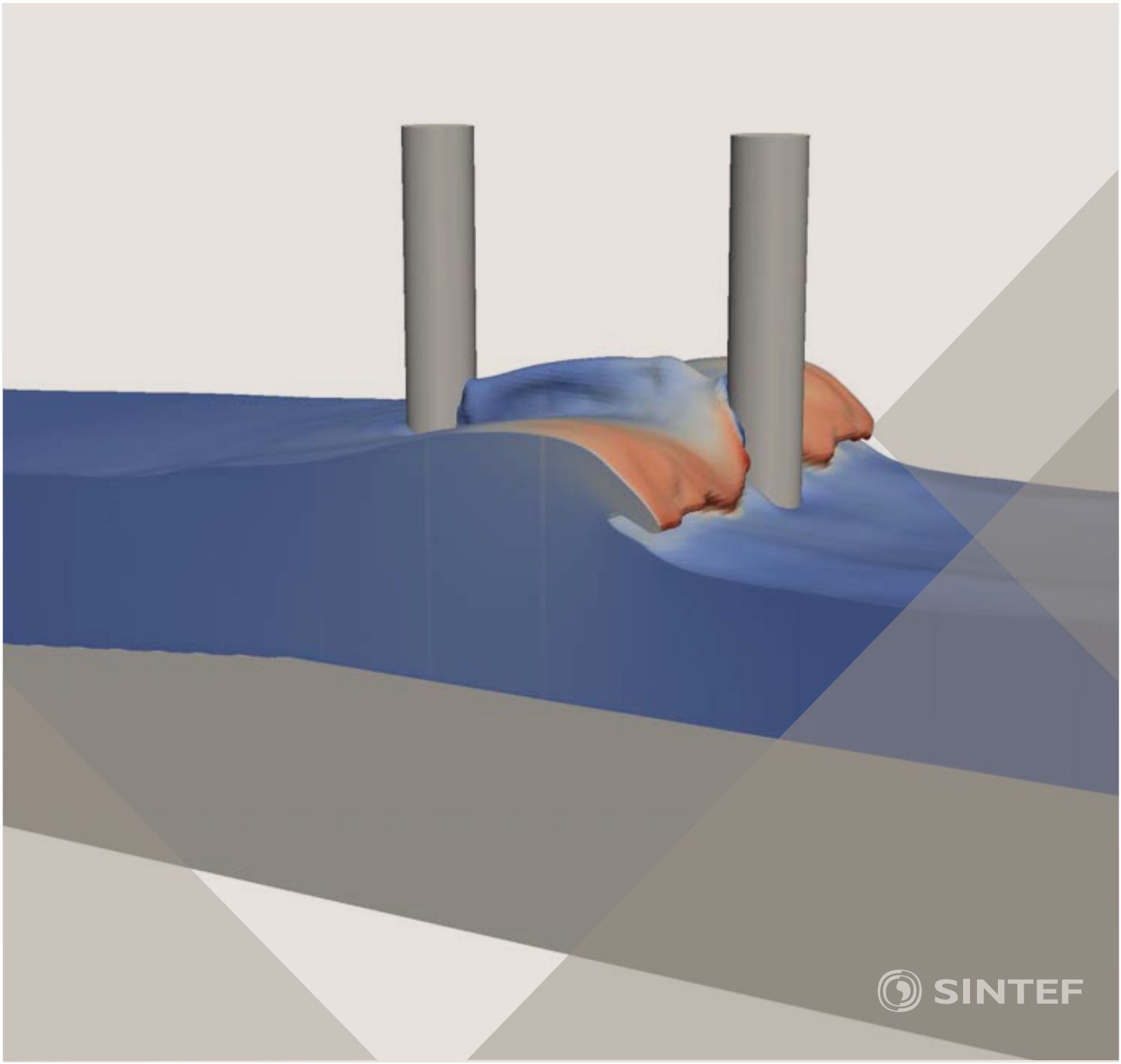

SINTEF Proceedings

Editors:
Jan Erik Olsen and Stein Tore Johansen

Progress in Applied CFD – CFD2017

Proceedings of the 12th International Conference on Computational Fluid Dynamics in the Oil & Gas, Metallurgical and Process Industries

SINTEF Academic Press

SINTEF Proceedings no 2
Editors: Jan Erik Olsen and Stein Tore Johansen
Progress in Applied CFD – CFD2017
Selected papers from 10th International Conference on Computational Fluid Dynamics in the Oil & Gas, Metallurgical and Process Industries

Key words:
CFD, Flow, Modelling

Cover, illustration: Arun Kamath

ISSN 2387-4295 (online)
ISBN 978-82-536-1544-8 (pdf)

SINTEF Academic Press
Address: Forskningsveien 3 B
PO Box 124 Blindern
N-0314 OSLO
Tel: +47 73 59 30 00
Fax: +47 22 96 55 08

www.sintef.no/byggforsk
www.sintefbok.no

SINTEF Proceedings
SINTEF Proceedings is a serial publication for peer-reviewed conference proceedings on a variety of scientific topics.
The processes of peer-reviewing of papers published in SINTEF Proceedings are administered by the conference organizers and proceedings editors. Detailed procedures will vary according to custom and practice in each scientific community.

PREFACE

This book contains all manuscripts approved by the reviewers and the organizing committee of the 12th International Conference on Computational Fluid Dynamics in the Oil & Gas, Metallurgical and Process Industries. The conference was hosted by SINTEF in Trondheim in May/June 2017 and is also known as CFD2017 for short. The conference series was initiated by CSIRO and Phil Schwarz in 1997. So far the conference has been alternating between CSIRO in Melbourne and SINTEF in Trondheim. The conferences focuses on the application of CFD in the oil and gas industries, metal production, mineral processing, power generation, chemicals and other process industries. In addition pragmatic modelling concepts and bio-mechanical applications have become an important part of the conference. The papers in this book demonstrate the current progress in applied CFD.

The conference papers undergo a review process involving two experts. Only papers accepted by the reviewers are included in the proceedings. 108 contributions were presented at the conference together with six keynote presentations. A majority of these contributions are presented by their manuscript in this collection (a few were granted to present without an accompanying manuscript).

The organizing committee would like to thank everyone who has helped with review of manuscripts, all those who helped to promote the conference and all authors who have submitted scientific contributions. We are also grateful for the support from the conference sponsors: ANSYS, SFI Metal Production and NanoSim.

Stein Tore Johansen & Jan Erik Olsen

Organizing committee:

Conference chairman: Prof. Stein Tore Johansen
Conference coordinator: Dr. Jan Erik Olsen
Dr. Bernhard Müller
Dr.Sigrid Karstad Dahl
Dr.Shahriar Amini
Dr.Ernst Meese
Dr.Josip Zoric
Dr.Jannike Solsvik
Dr.Peter Witt

Scientific committee:

Stein Tore Johansen, SINTEF/NTNU
Bernhard Müller, NTNU
Phil Schwarz, CSIRO
Akio Tomiyama, Kobe University
Hans Kuipers, Eindhoven University of Technology
Jinghai Li, Chinese Academy of Science
Markus Braun, Ansys
Simon Lo, CD-adapco
Patrick Segers, Universiteit Gent
Jiyuan Tu, RMIT
Jos Derksen, University of Aberdeen
Dmitry Eskin, Schlumberger-Doll Research
Pär Jönsson, KTH
Stefan Pirker, Johannes Kepler University
Josip Zoric, SINTEF

CONTENTS

CFD-DEM MODELLING OF BLAST FURNACE TAPPING

Mathias VÅNGÖ[1*], **Stefan PIRKER**[1], **Thomas LICHTENEGGER**[1,2]

[1]Department of Particulate Flow Modelling, Johannes Kepler University, 4040 Linz, AUSTRIA

[2]Linz Institute of Technology (LIT), Johannes Kepler University, 4040 Linz, AUSTRIA

[*] E-mail: mathias.vangoe@jku.at

ABSTRACT

The campaign length of a blast furnace is limited by the hearth inner lining lifetime. In order to maximize the campaign length and ensure a good draining of hot metal and slag, a good understanding of the flow in the hearth is essential. Challenges in modelling the flow involve several continuous phases (hot metal, slag and hot blast) as well as the presence of the deadman, a dense bed of coke particles. The shape and position of the deadman depend on the weight of the burden column above and the buoyancy forces from the liquids in the hearth.

A numerical coupled CFD (Computational Fluid Dynamics) – DEM (Discrete Element Method) model was developed and implemented in *CFDEMcoupling* (Goniva *et al.*, 2012), intended for future flow pattern investigation of the hearth during tapping. A VOF (Volume of Fluid) method is used to model the multiple continuous phases and DEM to model the discrete particles. The VOF and DEM models are coupled together in a 2-way manner, resulting in a complete 4-way coupled CFD-DEM model. We report the experimental validation of the model, performed on a small-scale particle filled tank. The tank was drained of water through the dense particle bed and the mass flow rate was measured.

Difficulties in choosing a fine enough mesh for the VOF method to correctly resolve the interface and simultaneously ensure a stable and accurate void fraction calculation arose. Different methods was proposed to enable particle sizes in the same range of the CFD cells, involving alternative methods for mapping the void fraction field onto the CFD mesh, as well as smoothing of the void fraction. With the smoothing model of Radl *et al.* (2014), the simulation was stable and very good agreements were found with the experimental measurements.

Keywords: VOF-method, DEM, multiphase flow, particle bed, blast furnace hearth .

NOMENCLATURE

Greek Symbols

α	volume fraction, $[-]$
ε	void fraction, $[-]$
ρ	density, $[kg/m^3]$
μ	dynamic viscosity / friction coefficient, $[kg/ms/-]$
ν	kinematic viscosity / Poisson's ratio, $[m^2/s/-]$
τ	viscous stress tensor, $[N/m^2]$
σ	surface tension, $[N/m]$
κ	interface curvature, $[1/m]$
ω	angular velocity, $[\mathrm{rad}/s]$
Δt	time step, $[s]$

Latin Symbols

$\mathbf{u}$	velocity, $[m/s]$.
p	pressure, $[Pa]$.
$p*$	non-hydrostatic pressure, $[Pa]$.
$\mathbf{g}$	gravity, $[m/s^2]$.
$\mathbf{x}$	coordinate, $[m]$.
$\mathbf{F}$	force, $[N]$.
m	mass, $[kg]$.
I	moment of inertia, $[kg\ m^2]$.
M	torque, $[Nm]$.
d	diameter, $[m]$.
V	volume, $[m^3]$.
COR	coefficient of restitution, $[-]$.
N	number of particles, $[-]$.

Sub/superscripts

f	fluid.
p	particle.
i	phase i / particle i.
c	compression.
σ	surface tension.
pf	particle-fluid interaction.
pp	particle-particle interaction.
T	turbulent.
$a.m$	added mass.
$semi-sat.$	semi-saturated.

INTRODUCTION

The blast furnace hearth condition has been proven to be critical to the campaign length as well as ensuring a stable operation. Increasing the blast furnace campaign length is of great importance because the re-lining is an expensive operation and causes a significant downtime in production (Shao, 2013; Zhang *et al.*, 2008). The hearth is an extremely harsh environment, temperatures exceeding 2000°C and high fluid velocities close to the tap holes cause great wear on the lining. Thus understanding the fluid flow pattern in the hearth is essential in order to optimize the campaign length (Ariyama *et al.*, 2014; Guo *et al.*, 2008).

The hearth is filled with liquid iron and slag, which settles in immiscible layers due to their different densities. Additionally, dense packed coke particles form a permeable structure often referred to as the deadman (Nnanna *et al.*, 2004; Tanzil *et al.*, 1984). The shape and position of the deadman depend on the operation, it is depending on the weight of the bur-

den column above and the buoyancy forces from the liquid metal and slag in the hearth. Due to the harsh environment, accurate measurements are difficult to perform, hence accurate models are essential in the understanding of the hearth (Huang *et al.*, 2005). In order to accurately model the tapping procedure it is important to consider the dynamics of the deadman.

Therefore, in this work a coupled CFD - DEM model was developed and implemented in the open-source software *CFDEMcoupling*, intended to be used in future work for flow pattern- and deadman dynamics investigation during tapping. In DEM, each individual particle is solved for, giving the model capabilities of accounting for the deadman dynamics at the expense of being extremely computationally demanding. The well known interface tracking method VOF (Hirt and Nichols, 1981; Gueyffier *et al.*, 1999), is used to model the multiple immiscible fluids.

MODEL DESCRIPTION

The CFD-DEM model is based on the theory for unresolved particle-fluid interaction, in which the flow around each particle is not resolved. Typically the CFD grid cells are larger than the particles and volume-averaged quantities are used on cell-size scale level. Sacrificing the smallest scale phenomena to solve for larger systems.

CFD governing equations

In order to model the multiple continuous phases, a VOF approach is used to track the interface. It is based on a mixture approach, where an indicator function ranging from 0 to 1 is used to distinguish between the fluids. The evolution of the interface is described by solving the advection equation,

$$\frac{\partial \alpha}{\partial t} + \nabla \cdot \left(\alpha \boldsymbol{u_f}\right) = 0, \tag{1}$$

where α is the volume fraction and $\boldsymbol{u_f}$ the fluid velocity (Hirt and Nichols, 1981; Li *et al.*, 1999). If the particle phase is considered as well as introducing a compression term to sharpen the interface, as done by Rusche (2002), a final set of transport equations for the volume fractions α_i can be written as,

$$\frac{\partial \varepsilon \alpha_i}{\partial t} + \nabla \cdot \left(\varepsilon \alpha_i \boldsymbol{u_f}\right) - \nabla \cdot \left(\boldsymbol{u_c} \alpha_i \left(1-\alpha_i\right)\right) = 0, \tag{2}$$

where ε is the local void fraction and $\boldsymbol{u_c}$ is the artificial compression velocity. The local fluid properties are determined by taking the volume weighted average of all the phases physical values as shown in Equation (3) and (4) for k continuous phases.

$$\rho_f = \sum_{i=1}^{k} \alpha_i \rho_i \tag{3}$$

$$\mu_f = \sum_{i=1}^{k} \alpha_i \mu_i \tag{4}$$

The flow is described by the Navier-Stokes (NS) equations in the form from Anderson and Jackson (1967). In VOF methodology only one momentum equation is solved, using the mixture fluid properties. Due to the presence of discrete particles, the void fraction term has been incorporated into the governing equations. The continuity equation is given by Equation (5) and the momentum equation by Equation (6).

$$\frac{\partial \varepsilon}{\partial t} + \nabla \cdot \left(\varepsilon \boldsymbol{u_f}\right) = 0 \tag{5}$$

$$\begin{aligned}\frac{\partial \varepsilon \rho_f \boldsymbol{u_f}}{\partial t} + \nabla \cdot \left(\varepsilon \rho_f \boldsymbol{u_f} \boldsymbol{u_f}\right) = &-\varepsilon \nabla p^* + \varepsilon \nabla \cdot \boldsymbol{\tau} - \varepsilon \left(\boldsymbol{g} \cdot \boldsymbol{x}\right) \nabla \rho_f \\ &+ \boldsymbol{F}^{\sigma} + \boldsymbol{F}^{pf}\end{aligned} \tag{6}$$

The formulation of pressure in Equation (6) is different from e.g. Anderson and Jackson (1967) and Sun and Sakai (2015). According to Rusche (2002), solving for a modified pressure p^*, defined as $p^* = p - \left(\boldsymbol{g} \cdot \boldsymbol{x}\right) \rho_f$, where $\boldsymbol{g}$ is the gravity vector and $\boldsymbol{x}$ the coordinate vector, simplifies the assignment of pressure boundary conditions as well as it offers a numerically better way of handling the strong density gradient at the interface. Physically, p^* can be interpreted as the pressure without the hydrostatic contribution. Furthermore, $\boldsymbol{\tau}$ denotes the viscous stress tensor, which is usually written as $\boldsymbol{\tau} = \mu_f \left(\nabla \boldsymbol{u}_f + \nabla \boldsymbol{u}_f^T\right)$. F^{σ} is the surface tension force, defined as $F^{\sigma} = \sigma \kappa \nabla \alpha$, where σ denotes the surface tension and κ is the interface curvature. $\boldsymbol{F}^{pf}$ is a source term arising from the momentum exchange between the fluids and particles, which is further described in the following section.

DEM governing equations

The discrete particles are described with DEM. It is a well known numerical method for solving granular flows and it is based on the theory of Cundall and Strack (1979). Each particle is solved individually by determining its trajectory with Newton's laws of motion as,

$$m_i \frac{d\boldsymbol{u}_{p,i}}{dt} = \boldsymbol{F}_i^{pp} + \boldsymbol{F}_i^{pf} + m_i \boldsymbol{g}, \tag{7}$$

$$I_i \frac{d\boldsymbol{\omega}_{p,i}}{dt} = \boldsymbol{M}_i^{pp} + \boldsymbol{M}_i^{pf}, \tag{8}$$

where $\boldsymbol{u}_{p,i}$ is the particle velocity and $\boldsymbol{\omega}_{p,i}$ the angular velocity. $\boldsymbol{F}_i^{pp}$ denotes the inter-particle force and F_i^{pf} the particle-fluid interaction force. In this work, relatively large particles are used ($d_p \sim O(10^{-3} m)$), thus neglecting any cohesive forces which can be important for e.g. powders. The particle-particle interaction term is then described only by the collision forces.

The particle-fluid interaction term, $\boldsymbol{F}_i^{pf}$, is fully defined as:

$$\begin{aligned}\boldsymbol{F}_i^{pf} = &\boldsymbol{F}_{drag,i} + \boldsymbol{F}_{\nabla p,i} + \boldsymbol{F}_{\tau,i} + \boldsymbol{F}_{Basset,i} + \boldsymbol{F}_{a.m,i} \\ &+ \boldsymbol{F}_{Saffman,i} + \boldsymbol{F}_{Magnus,i},\end{aligned} \tag{9}$$

where the components on the right hand side are respectively the drag force, pressure gradient force, viscous force, Basset force, added-mass force, Saffman- and Magnus-lift force. In this work, the Basset-, added-mass-, Saffman- and Magnus-forces are neglected because it is expected that the drag-, pressure gradient- and viscous-forces are dominant (Zhou *et al.*, 2010). Equation (7) can then be rewritten as,

$$m_i \frac{d\boldsymbol{u}_{p,i}}{dt} = \sum_{i=1}^{n} \boldsymbol{F}_i^{contact} + \boldsymbol{F}_{drag,i} + \boldsymbol{F}_{\nabla p,i} + \boldsymbol{F}_{\tau,i} + m_i \boldsymbol{g}, \tag{10}$$

where $\boldsymbol{F}_{\nabla p,i} = -V_{p,i} \nabla p$ and $\boldsymbol{F}_i = V_{p,i} \nabla \cdot \boldsymbol{\tau}$. In this work the Koch and Hill drag model (Hill *et al.*, 2001; van Buijtenen *et al.*, 2011) was used.

Smoothing

One contradiction arises due to the nature of the model. In VOF methodology, a fine mesh is desired to resolve the interface, where as for unresolved CFD-DEM, the cell size should be larger than the particles in order to accurately map the void fraction field onto the mesh. A few alternative methods for calculating the void fraction have been suggested to enable for particle sizes in the range of the cell sizes. For example, Jing (2016) used an approach where the particles are artificially enlarged to influence more surrounding cells, while keeping the volume constant.
Additionally, Peng *et al.* (2014) reported that, small inaccuracies in mapping the void fraction onto the mesh eventually causes local pressure fluctuations due to the formulation of the governing equations. Reducing these fluctuations is of great importance in order to ensure stable simulations. Additional treatment of the exchange fields can be performed to improve stability, as done by e.g. Pirker *et al.* (2011), Radl *et al.* (2014) and Capecelatro and Desjardins (2013), where a diffusion equation,

$$\frac{\partial \phi}{\partial t} = D\nabla^2\phi, \tag{11}$$

for the quantity in question ϕ is solved. D is the diffusion coefficient, which can be defined as $D = l^2/\Delta t$, where l is interpreted as the smoothing length. By performing this operation, the exchange fields are "smeared" over nearby cells.

EXPERIMENTAL SETUP

The tank was a transparent box with the dimensions 330x150x400 mm. A cylindrical tap hole with the diameter $d_{outlet} = 27.5$ mm was located at the bottom of the side. A schematical view of the setup is shown in Figure 1. A valve was used to control the tapping and the total bulk mass tapped was measured with a load cell. Because coke particles are buoyant in the blast furnace hearth, wood particles were chosen in order to be buoyant in water. The measured particle properties are listed in Table 1. As a result of choosing wooden particles, the particle properties varied between wet or dry because the wood soaked water. The particles were measured and weighed in between ten experimental runs. A semi-saturated state of the particles was reached after five instances where-after for the following five runs, the particle-diameter and density were determined to $d_p = 6.5$ mm and $\rho_p = 850\ \mathrm{kg/m^3}$ respectively.

Table 1: Particle properties

N_p	40000
$\rho_{p,dry}$	600 kg/m^3
$\rho_{p,semi-sat.}$	850 kg/m^3
$d_{p,dry}$	6.0 mm
$d_{p,semi-sat.}$	6.5 mm

For a first test run, a sitting particle bed was considered. The initial water level was set to 300 mm and the buoyant particles were held down by a grid as shown in Figure 1. Another grid was placed at the outlet to hinder the particles from leaving the tank.

SIMULATION SETUP

The computational domain is shown in Figure 2. Its outer dimensions are 330x150x350 mm and it is divided in 1920 hexahedral cells, with the smallest cell size, $\Delta x_{min} = 11$ mm

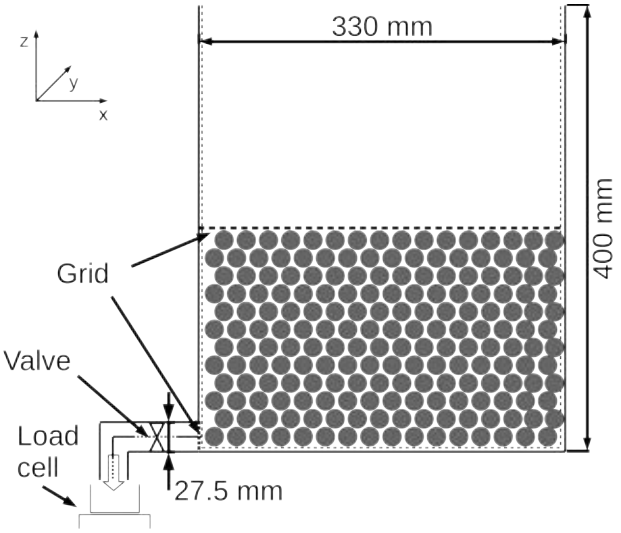

Figure 1: Schematic diagram of the experimental setup.

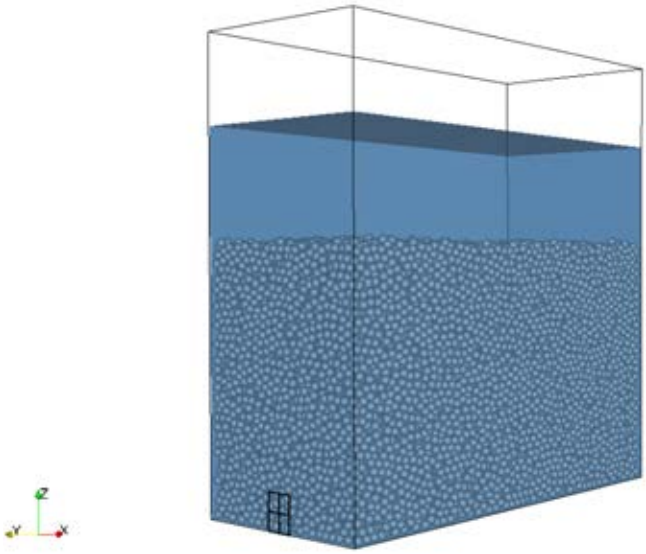

Figure 2: Computational domain and the initial state of the particle bed and water level.

and the biggest, $\Delta x_{max} = 25$ mm. It should be noted that a few assumptions were made to the tap hole. In the simulation, the tap hole was modeled as a square instead of a circle with the side, a, calculated as:

$$a = \frac{1}{2}\sqrt{\pi d_{outlet}^2}, \tag{12}$$

Additionally, the pipe from the experimental setup was not modeled in the simulation. Thus it was assumed that the pipe pressure drop could be neglected. Figure 2 also shows the initial state the simulation. In order to ensure that the particles remain on the bottom, the particle density is set to 2500 kg/m^3. The full list of simulation parameters are listed in Table 2 and 3, where ν_p denotes the Poisson's ratio, COR the coefficient of restitution and μ_p the friction coefficient. It should be noted that the particle time step size was 100 times smaller than the fluid time step, meaning that 100 sub-iterations of DEM calculations were performed for every CFD time step.

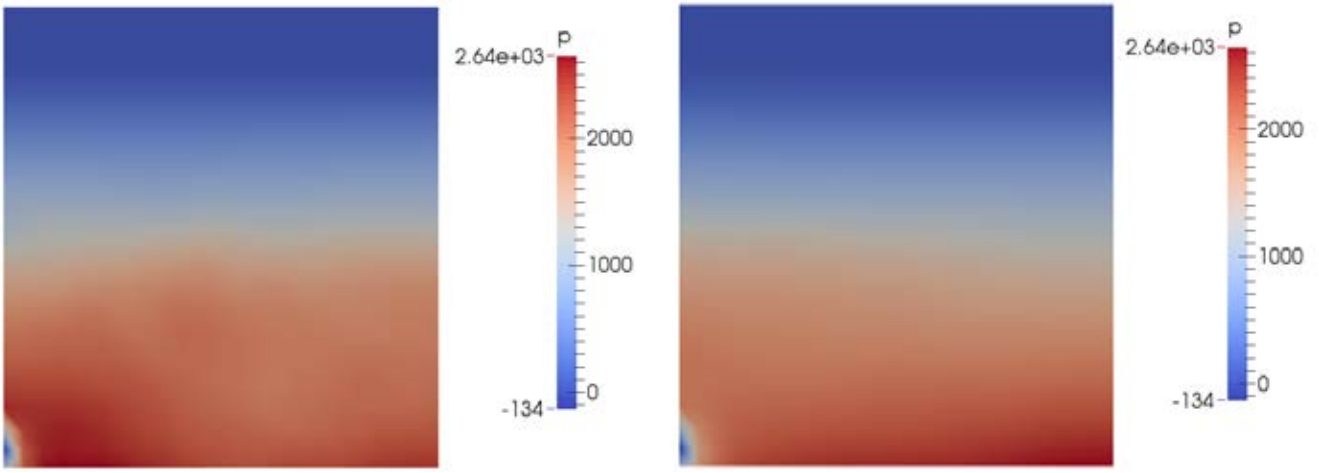

(a) Unsmoothed, t = 1 s

(b) Smoothed, t = 1 s

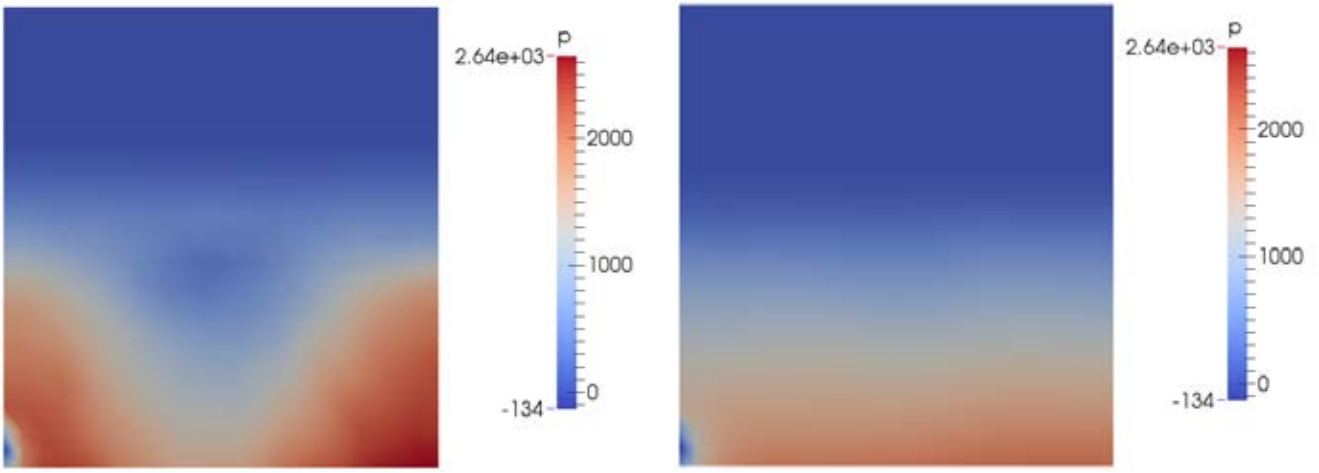

(c) Unsmoothed, t = 15 s

(d) Smoothed, t = 15 s

Figure 3: Pressure for the unsmoothed- (left) and smoothed (right) simulation at the central plane for various time steps.

Table 2: Simulation parameters: fluid

Δt_f	$5 \cdot 10^{-3}$ s
ρ_{water}	1000 kg/m^3
ρ_{air}	1.0 kg/m^3
ν_{water}	$1.0 \cdot 10^{-6}$ m^2/s
ν_{air}	$1.0 \cdot 10^{-5}$ m^2/s
$\sigma_{water-air}$	0.07 N/m

Table 3: Simulation parameters: particle

Δt_p	$5 \cdot 10^{-5}$ s
ρ_p	**2500** kg/m^3
d_p	6.5 mm
N_p	40000
Young's modulus	$5 \cdot 10^{-6}$ Pa
ν_p	0.45
COR	0.3
μ_p	0.5

RESULTS

The effect of smoothing on the pressure is depicted in Figure 3. Two different simulations were carried out, one unsmoothed and one with the smoothing model previously described active with the smoothing length $l = 3d_p$. The top row shows the resulting pressure at $t = 1$ s and the bottom row at $t = 15$ s. One would expect a linearly increasing pressure towards the bottom due to the hydrostatic pressure. Consequently, the maximum pressure at the bottom would decrease as the water level decreased. The expected behavior can be observed in the smoothed simulation, while the pressure in the unsmoothed shows an odd behavior. Thus, validation was performed with the smoothing model active.
Figure 4 illustrates the instantaneous flow field at $t = 8$ s. Due to atmospheric pressure at the outlet, the fluid is drained and high fluid velocities are observed at the outlet. The monitored mass flow rate is shown in Figure 5 . As expected, the mass flow rate was high at the beginning and decreased over time as the water level decreased and the tank was fully drained after approximately 80 s. In order to compare the simulation with the experimental results, the mass flow rate was integrated over time. It is depicted in Figure 6 together with the measurements. The experimental data is presented by error bars, which represents the minimum-, mean- and maximum-value of five experimental runs (as motivated in the previous section). The dotted line represents the initial

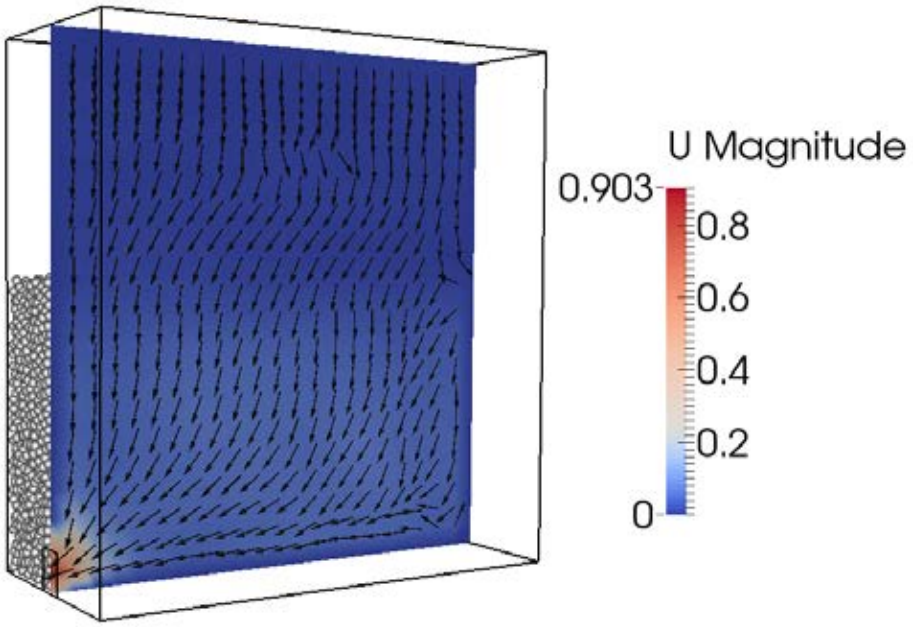

Figure 4: Illustration of the flow field at $t = 8$ s.

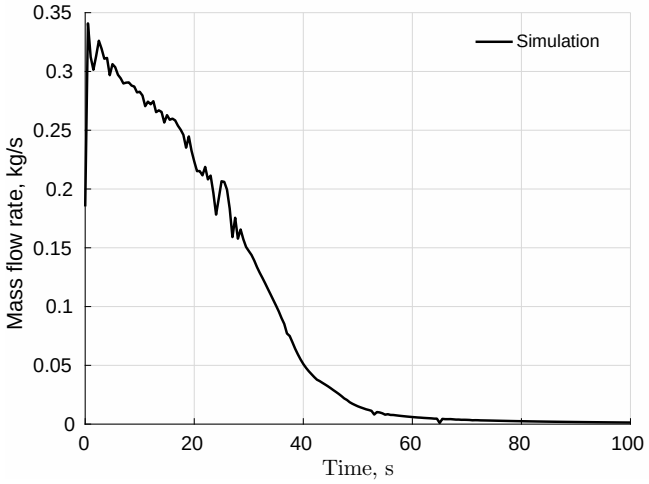

Figure 5: Tapping mass flow rate over time for a simulation of the experimental setup.

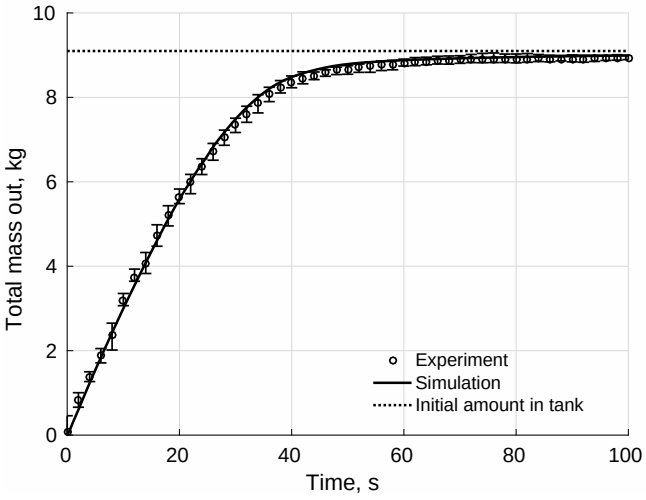

Figure 6: Integrated mass flow rate over time, compared with experimental measurements.

amount of water in the tank.

It can be seen that the simulation successfully reproduced the drainage pattern observed in the experiments. Both the simulation result and the measurements converged towards the expected amount drained and a small liquid hold up was noticeable in the experiments as well as in the simulations.

CONCLUSION

A VOF-DEM coupled solver was successfully implemented in the open-source software *CFDEMcoupling*, with capabilities of handling n continuous phases in conjunction with discrete particles.

A tank-draining experiment was set up to provide experimental measurements to validate the model. Water was drained through a sitting particle bed, consisting of wooden particles and the flow rate was measured.

Numerical instabilities were encountered due to a relatively fine mesh. Alternative ways of calculating the void fraction, as well as smoothing of the exchange fields were performed with success. With the smoothing model of Radl *et al.* (2014), very good agreement was found for the mass flow rate compared to the experimental measurements.

REFERENCES

ANDERSON, T.B. and JACKSON, R.O.Y. (1967). "A Fluid Mechanical Description of Fluidized Beds". *Industrial & Engineering Chemistry Fundamentals*, **6(4)**, 527–539.

ARIYAMA, T., NATSUI, S., KON, T., UEDA, S., KIKUCHI, S. and NOGAMI, H. (2014). "Recent Progress on Advanced Blast Furnace Mathematical Models Based on Discrete Method". *ISIJ International*, **54(7)**, 1457–1471.

CAPECELATRO, J. and DESJARDINS, O. (2013). "An Euler-Lagrange strategy for simulating particle-laden flows". *Journal of Computational Physics*, **238**, 1–31.

CUNDALL, P.A. and STRACK, O.D.L. (1979). "A discrete numerical model for granular assemblies". *Géotechnique*, **29(1)**, 47–65.

GONIVA, C., KLOSS, C., DEEN, N.G., KUIPERS,

J.A.M. and PIRKER, S. (2012). "Influence of rolling friction on single spout fluidized bed simulation". *Particuology*, **10(5)**, 582–591.

GUEYFFIER, D., LI, J., NADIM, A., SCARDOVELLI, S. and ZALESKI, S. (1999). "Volume of fluid interface tracking with smoothed surface stress methods for three-dimensional flows". *J. Comput. Phys.*, **152**, 423–456.

GUO, B.Y., MALDONADO, D., ZULLI, P. and YU, A.B. (2008). "CFD Modelling of Liquid Metal Flow and Heat Transfer in Blast Furnace Hearth". *ISIJ International*, **48(12)**, 1676–1685.

HILL, R.J., KOCH, D.L. and LADD, A.J.C. (2001). "The first effects of fluid inertia on flows in ordered and random arrays of spheres". *Journal of Fluid Mechanics*, **448(2001)**, 243–278.

HIRT, C.W. and NICHOLS, B.D. (1981). "Volume of fluid (VOF) method for the dynamics of free boundaries". *Journal of Computational Physics*, **39(1)**, 201–225.

HUANG, D.F., YAN, F., MILLOVACHI, P., CHAUBAL, P. and ZHOU, C.Q. (2005). "Numerical Investigation of Transient Hot Metal Flows in a Blast Furnace Hearth". *Aistech 2005*, **I(1)**, 199–207.

JING, L. KWOK, C.L.Y.S.Y.D. (2016). "Extended CFD-DEM for free-surface flow with multi-size granules". *International Journal for Numerical and Analytical Methods in Geomechanics*, **40**, 62–79.

LI, Y., ZHANG, J. and FAN, L.S. (1999). "Numerical simulation of gas–liquid–solid fluidization systems using a combined CFD-VOF-DPM method: bubble wake behavior". *Chemical Engineering Science*, **54(21)**, 5101–5107.

NNANNA, A.G.A., ULUDOGAN, A., ROLDAN, D. and ZHOU, C.Q. (2004). "Water Model of a Blast Furnace Hearth for Flow Pattern Investigation". *AISTech 2004 Proceedings*, vol. I, 35–46.

PENG, Z., DOROODCHI, E., LUO, C. and MOGHTADERI, B. (2014). "Influence of Void Fraction Calculation on Fidelity of CFD-DEM Simulation of Gas-Solid Bubbling Fluidized Beds". *AIChE Journal*, **60(6)**, 2000–2018.

PIRKER, S., KAHRIMANOVIC, D. and GONIVA, C. (2011). "Improving the applicability of discrete phase simulations by smoothening their exchange fields". *Applied Mathematical Modelling*, **35(5)**, 2479–2488.

RADL, S., GONZALEZ, B., GONIVA, C. and PIRKER, S. (2014). "State of the Art in Mapping Schemes for Dilute and Dense Euler-Lagrange Simulations". *10th International Conference on CFD in Oil & Gas, Metallurgical and Process Industries*, **(June)**, 1–9.

RUSCHE, H. (2002). *Computational Fluid Dynamics of Dispersed Two-Phase Flows at High Phase Fractions*. Ph.D. thesis, Imperial College of Science, Technology & Medicine.

SHAO, L. (2013). *Model-Based Estimation of Liquid Flows in the Blast Furnace Hearth and Taphole*. Ph.D. thesis, Åbo Akademi University.

SUN, X. and SAKAI, M. (2015). "Three-dimensional simulation of gas–solid–liquid flows using the DEM–VOF method". *Chemical Engineering Science*, **134**, 531–548.

TANZIL, W., ZULLI, P., BURGESS, J.M. and V., P.W. (1984). "Experimental Model Study of the Physical Mechanisms Governing Blast Furnace Hearth Drainage". *Transactions of the Iron and Steel Institute of Japan*, **24(3)**, 197–205.

VAN BUIJTENEN, M.S., VAN DIJK, W.J., DEEN, N.G., KUIPERS, J., LEADBEATER, T. and PARKER, D. (2011). "Numerical and experimental study on multiple-spout fluidized beds". *Chemical Engineering Science*, **66(11)**, 2368–2376.

ZHANG, Y., DESHPANDE, R., HUANG, D.F., CHAUBAL, P. and ZHOU, C.Q. (2008). "Numerical analysis of blast furnace hearth inner profile by using CFD and heat transfer model for different time periods". *International Journal of Heat and Mass Transfer*, **51(1-2)**, 186–197.

ZHOU, Z.Y., KUANG, S.B., CHU, K.W. and YU, A.B. (2010). "Discrete particle simulation of particle–fluid flow: model formulations and their applicability". *Journal of Fluid Mechanics*, **661**, 482–510.